CROATICA CHEMICA ACTA
CCACAA, ISSN-0011-1643, ISSN-1334-417X
Croat. Chem. Acta **82** (1) (2009) 115−127.
CCA-3301

Original Scientific Paper

DFT Studies on Molecular and Electronic Structures of Cationic Carbene Complexes $[L_2(\eta^5\text{-}C_5H_5)Fe{=}CR_2]^+$ (L = CO, PH_3, dhpe, PPh_3; R = H, F, CH_3)*

Isabella Hyla-Kryspin, Christian Mück-Lichtenfeld, and Stefan Grimme****

Organisch-Chemisches Institut der Universität Münster, Corrensstr. 40, D-48149 Münster, Germany

RECEIVED JUNE 18, 2008; REVISED SEPTEMBER 19, 2008; ACCEPTED SEPTEMBER 22, 2008

Abstract. For the title complexes we discuss the results of DFT calculations for (i) the molecular and electronic structures, (ii) the rotational barriers of the carbenes around the Fe=C_{carb} bond (ΔE_{rot}), and (iii) the binding energies of the carbenes (D_e). Where available, the calculated properties of the Fe=C_{carb} bonds are compared with previous theoretical and experimental data of some prototypical carbene complexes classified as Fischer- or Schrock-type compounds. It is shown that the rotational barriers of the carbenes, the Fe−C_{carb} bond distances and bond strengths are sensitive to the carbene substituents and to the ligands L attached to iron. For complexes with given L the values of ΔE_{rot} diminish in the order: $CH_2 > CF_2 > CMe_2$ and an inverse ordering is obtained for the decrease of the Fe=C_{carb} bond distance. The ΔE_{rot} of dimethylcarbene are close to those of Fischer-type compounds, while ΔE_{rot} of methylidene approach values typical for Schrock-type carbenes. The replacement of the CO ligand by poorer π-acceptor ligand increases the values of ΔE_{rot} in the order: CO < PH_3 < dhpe < PPh_3 and diminishes the Fe−C_{carb} bond distance in the same order. The binding energies (D_e) of the carbenes are larger than the first dissociation energy of CO from the pentacarbonyliron complex. For complexes with given L, except one, the D_e values decrease in the order: $CH_2 > CMe_2 > CF_2$. The properties of the investigated compounds are traced back to the character of the Fe → C_{carb} π-backbonding interactions and their competitions with the Fe → L and R → C_{carb} π-interactions. It is also shown that the PH_3 ligand can only be considered with caution as a good model for the PPh_3 ligand in computational studies.

Keywords: iron carbenes, rotational barriers, binding energies, DFT calculations

INTRODUCTION

Since the first syntheses of the transition metal (TM) carbene complexes,[1] the chemistry of these compounds was rapidly developing.[2] This was mainly due to the potential of TM carbenes to mediate novel C−C bond-forming reactions in a wide range of important organometallic catalytic processes and organic syntheses, ranging from alkene metathesis and polymerizations[3] to biochemical oxidation[4] and cyclopropanation reactions.[5]

With respect to the specific reactivity, TM carbenes, $L_nTM{=}C(R)R'$, are generally classified as Fischer- or Schrock-type compounds.[2,6] Both classes of compounds have been the subject of intense theoretical studies focusing on molecular and electronic structures and first of all on the nature of the TM carbene carbon bond.[7−11] In Fischer complexes the ligated carbene carbon acts as electrophile toward other chemical reagents, while in Schrock complexes it is nucleophilic. The carbene ligand in Fischer complexes typically possesses a stabilizing π-donor substituent (*e.g.* R; R' = OR, NR_2) and the TM is in a low oxidation state. The TM-carbene bond of Fischer compounds is usually discussed in terms of the Dewar-Chatt-Duncanson model[12] concerning the donor acceptor interactions between carbenes and metal fragments, both in the singlet state (Scheme 1a).[8c,9a,10a−c,10f−i] In Schrock complexes the TM is in a high oxidation state and the carbene ligand did not have a stabilizing π-donor substituent. The TM-carbene interaction in Schrock complexes is usually described as a covalent double bond between the triplet state of the carbene and the triplet state of the TM-fragment (Scheme 1b).[8d−g,9a,10g,h] Since in Schrock carbenes the substituents R and R' are H or alkyl, they are also referred to as TM alkylidenes.

It should be noticed however, that the oxidation state of the TM as well as the presence or absence of the heterosubstituents in the carbene ligand are not always a

* Dedicated to Professor Zvonimir Maksić on the occasion of his 70th birthday.
** Authors to whom correspondence should be addressed. (E-mail: grimmes@uni-muenster.de; ihk@uni-muenster.de)

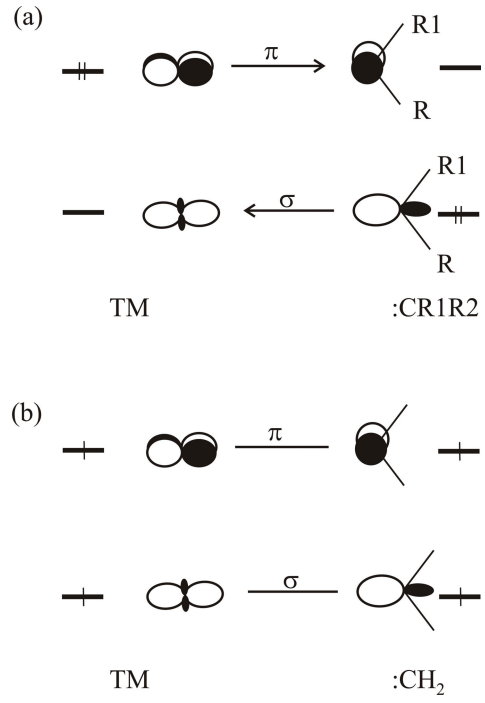

Scheme 1.

safe criterion for predicting nucleophilic or electrophilic reactivity.[13] Thus, for example, for the prototype cationic methylidene complexes with metals from groups 6, 7, and 8 it was shown that they contain an electrophilic carbene center.[5a,14]

In the present work we are interested in the structural and bonding properties of the cationic carbene complexes with a general formula $[L1L2(\eta^5\text{-}C_5H_5)Fe{=}C(R)R']^+$ (L1, L2 = σ-bonding ligand; R, R' = H, alkyl) which according to their reactivity should be classified as Fischer-carbenes, despite the alkylidene nature of the carbene ligands and the formal Fe^{II} oxidation state of iron. Among them the cationic alkylidene complexes $[(CO)_2(\eta^5\text{-}C_5H_5)Fe{=}C(R)R']^+$ (R, R' = H, alkyl) are one of the most reactive carbenes. In most cases their existence could be only implied by the transfer of the carbene moiety to an olefin substrate resulting in cyclopropane formation, as proposed for the first time by Pettit and Jolly in 1966 for the $[(CO)_2(\eta^5\text{-}C_5H_5)Fe{=}CH_2]^+$ complex.[5a] Due to the high reactivity, only few examples of cationic dicarbonylcyclopentadienyl-iron-carbene complexes were isolated or at least spectroscopically characterized. They include the dimethylcarbene complex $[(CO)_2(\eta^5\text{-}C_5H_5)Fe{=}CMe_2]^+$,[15] the benzylidene complex $[(CO)_2(\eta^5\text{-}C_5H_5)Fe{=}CHPh]^+$,[16] and the cyclopropylmethylidene complex $[(CO)_2(\eta^5\text{-}C_5H_5)Fe{=}CH(c\text{-}C_3H_5)]^+$.[17] The crystallographic data of these complexes are not known.

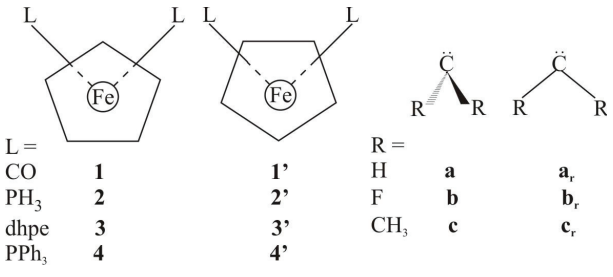

Scheme 2.

The reactivity and stability of the cationic iron-carbene complexes is highly sensitive to the environment of the metal. The substitution of one or two carbonyl ligands by the PMe_3, PPh_3 or the dppe (dppe = 1,2-bis(diphenylphosphane)ethane) ligands as well as of the C_5H_5 ligand by the C_5Me_5 one, generally results in a thermally stable species.[16b,18] To our best knowledge, among the $[L1L2(\eta^5C_5Me_5)Fe{=}CR(R')]^+$ complexes (R, R' = H, alkyl), only the $[(dppe)(C_5Me_5)Fe{=}C(H)Me][PF_6]$ compound was characterized by X-ray crystallography.[18b]

In the present work we would like to describe (i) the molecular and electronic structures of the iron-carbene complexes, $[L1L2(\eta^5\text{-}C_5H_5)Fe{=}CR_2]^+$ (L1, L2 = CO, PH_3, 1,2-bis(dihydrophosphane)ethane (dhpe), PPh_3; R = H, F, CH_3), (ii) the binding energies of the carbene ligands, and (iii) the rotational barriers of the carbenes around the iron carbene bond. We are interested in the question how the replacement of the CO ligand by a poorer π-acceptor one changes the character of the iron carbene carbon bond as well as whether the PH_3 ligand, which is frequently used in theoretical investigations as a model of bulky organophosphanes is a good substituent for the PPh_3 ligand, which is more common in experimental studies. The complexes are labeled with respect to the cyclopentadienyl rotamers of the complex fragments $L1L2(\eta^5\text{-}C_5H_5)Fe^+$ (L1, L2 = CO (**1**, **1'**), PH_3 (**2**, **2'**), dhpe (**3**, **3'**), PPh_3 (**4**, **4'**)) as well as to the spatial coordination the carbene ligands $:CR_2$ (R = H (**a**, $\mathbf{a_r}$), F (**b**, $\mathbf{b_r}$), CH_3 (**c**, $\mathbf{c_r}$)) (Scheme 2). The dhpe ligand models the computationally more demanding dppe one.

To our knowledge, among the compounds under study only the $[(CO)_2(\eta^5\text{-}C_5H_5)Fe{=}CH_2]^+$ complex (**1a**) was theoretically investigated so far.[7c] On the basis of semiempirical Extended-Hückel calculations it was possible to characterize the origin of the methylidene rotational barrier. For **1a** and $\mathbf{1a_r}$ the authors found that the rotational barrier of the methylidene ligand is traced back to the π-backbonding interaction which in the former complex is stronger.[7c] It is clear that a more accurate and quantitative description of the structural and electronic properties of the iron-carbene complexes could not be achieved within the Extended-Hückel scheme. Thus, our choice of the ligands as well as of the density functional approach should give a quantitative insight into the structural and electronic properties of the investigated species.

CALCULATIONS DETAILS

All calculations were performed with the TURBOMOLE 5.7 package of programs.[19] Since all investigated complexes can be considered as low-spin, d^6 pseudooctahedral species, the geometry optimizations of the complexes $[L_2(\eta^5\text{-}C_5H_5)Fe{=}CR_2]^+$ (L = CO, PH_3, PPh_3, dhpe; R = H, CH_3, F) and their molecular fragments $L_2(\eta^5\text{-}C_5H_5)Fe^+$ were carried out for the singlet states. The carbenes $:CR_2$ were optimized in the singlet and triplet states. In our calculations the dhpe ligand ($PH_2CH_2CH_2PH_2$) possesses H atoms instead of the phenyl groups in the experimental dppe ligand ($Ph_2PCH_2CH_2PPh_2$). As main quantum chemical method we have chosen the density functional theory (DFT)[20] with the gradient-corrected BP86 functional[21] and the RI approximation which takes advantage of density fitting for the calculations of the Coulomb integrals.[22] All atoms were described with an all-electron valence triple-zeta basis set augmented with polarization function: (17s11p6d1f)/[6s4p3d1f] for Fe, (14s9p1d)/[5s4p1d] for P, (11s6p1d)/[5s3p1d] for C, O, and F, and (5s1p)/[3s1p] for H, which we denote as TZVP. Few calculations were also carried out by using larger TZVPP basis sets as well as the B97-D[23] and B3LYP[24] functionals with the TZVP basis. In the TZVPP basis sets f and d polarization functions are added to the TZVP basis sets of C, O, F, P and H, respectively. The basis sets, together with the corresponding auxiliary basis sets for the RI approximation, were taken from the TURBOMOLE basis set library in the subdirectories basen and jbasen, respectively.[19]

The dissociation energy of the carbene ligands is calculated as:

$$D_e = \Delta E = (E_1 + E_2) - E_{comp} \quad (1)$$

E_{comp}, E_1, and E_2 are the total energies of the lowest energy equilibrium ground state structures of the carbene complexes $[L_2(\eta^5\text{-}C_5H_5)Fe{=}CR_2]^+$, the metal fragments $L_2(\eta^5\text{-}C_5H_5)Fe^+$, and the carbene ligands, respectively. In order to obtain deeper insight into iron-carbene bonding the dissociation energy, ΔE, was partitioned into the relaxation energies $\Delta E_{rel}(1)$ and $\Delta E_{rel}(2)$ and the intrinsic dissociation energy ΔE_i .

$$\Delta E = \Delta E_i + \Delta E_{rel}(1) + \Delta E_{rel}(2) \quad (2)$$

The intrinsic dissociation energy, ΔE_i, corresponds to the dissociation process into the molecular fragments with geometries that they adopted in the complexes, and $\Delta E_{rel}(1)$ and $\Delta E_{rel}(2)$ are, respectively, the relaxation energies of the $L_2(\eta^5\text{-}C_5H_5)Fe^+$ ant the $:CR_2$ molecular fragments from complex geometries to their ground state equilibrium structures. This partitioning scheme allows also correcting the intrinsic dissociation energy (ΔE_i) and, consequently, the total dissociation energy (ΔE) for basis set superposition error (BSSE). The BSSE was calculated according to the counterpoise procedure[25] and the corrected energies are denoted as ΔE_i^{CP} and ΔE^{CP} (Eq. 3).

$$D_e = \Delta E^{CP} = \Delta E_i^{CP} + \Delta E_{rel}(1) + \Delta E_{rel}(2) \quad (3)$$

Finally, the bonding properties of the carbene ligands were also investigated with the help of NPA and NBO population analyses.[26]

RESULTS AND DISCUSSION

Molecular Structures and Rotational Barriers

The optimized structures of the complexes under study adopt C_s symmetry. In **1a-c** – **4a-c** and **1'a-c** – **4'a-c** the carbene substituents lie in the symmetry plane going through the carbene carbon atom, the iron atom and the middle of the cyclopentadienyl ligand. In the remaining structures they are rotated by 90º around the iron carbene carbon bond. For the sake of clarity, the optimized structures of **1a-c** – **4a-c** are shown in Figure 1 and those of **1a**, $\mathbf{1a_r}$, **1'a**, and $\mathbf{1'a_r}$ together with the number of the imaginary frequencies (NIMAG) are depicted in Figure 2 as an example. According to the vibrational analyses, all frequencies are real for **1a-c** – **4a-c** and consequently these structures represent minima on their potential energy surfaces. With respect to **1a-c** – **4a-c** the structures **1'a-c** – **4'a-c** and $\mathbf{1a_r}$-$\mathbf{c_r}$ – $\mathbf{4a_r}$-$\mathbf{c_r}$ represent, respectively, the rotamers of the cyclopentadienyl and the carbene ligands. In $\mathbf{1'a_r}$-$\mathbf{c_r}$ – $\mathbf{4'a_r}$-$\mathbf{c_r}$ a coupled rotation of the cyclopentadienyl and the carbene ligand occurs.

The relative energies of all optimized structures are presented in Table 1. Table 2 provides the results of the NPA and NBO population analyses for the global minimum structures **1a-c** – **4a-c** and the lowest energy carbene rotamers together with the rotational barriers. Selected optimized parameters of **1a-c** – **4a-c** and of the corresponding carbene rotamers are collected in Table 3. The optimized parameters of the metal fragments $L_2(\eta^5\text{-}C_5H_5)Fe^+$ (L = CO (**1**), PH_3 (**2**), PPh_3 (**4**); 2L = dhpe (**3**)) and of the free carbenes $:CR_2$ (R = H (**a**), F (**b**), CH_3 (**c**)) are provided in Table 4. We notice that it was not possible to optimize **2'a** and $\mathbf{4'a_r}$ with η^5-bonded cyclopentadienyl ligand. During the geometry optimizations these conformers converged to structures in which the cyclopentadienyl ligand is η^1- (**2'a**) or η^2- ($\mathbf{4'a_r}$) bonded (Scheme 3). Taking into account the dif-

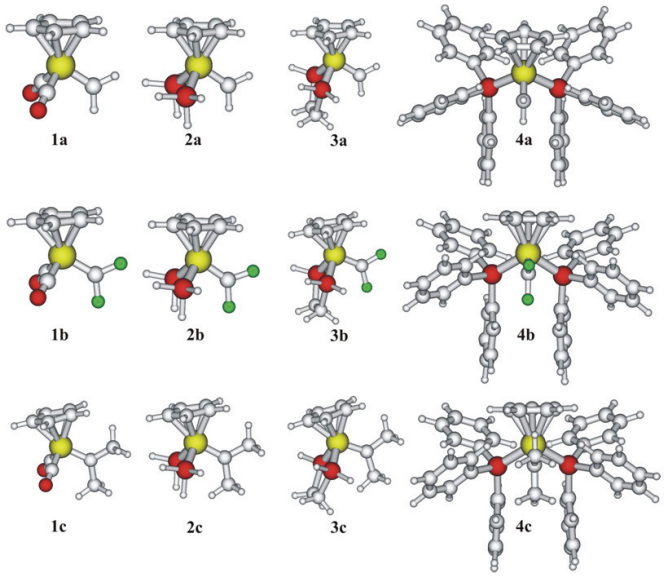

Figure 1. Optimized structures of the global minima **1a-c** – **4a-c**.

ferent manner of the iron-cyclopentadienyl bonding, both structures are not discussed here.

For **4a-c**, **3a**, and **3b** the lowest energy carbene rotamers correspond to structures **4a$_r$-c$_r$**, **3a$_r$**, and **3b$_r$**, while for **1a-c**, **2a-c**, and **3c** they are the structures **1'a$_r$-c$_r$**, **2'a$_r$-c$_r$**, and **3'c$_r$** in which a coupled rotation of the carbene and the cyclopentadienyl ligand occurs (Table 1).

The question of the rotational barrier around the transition metal carbene carbon bond has stimulated some experimental and theoretical investigations. On the basis of Hartree-Fock,[8c,8e] CASSCF,[9c] and DFT[10b] calculations it was recognized that the rotation around the TM=C$_{carb}$ bond is essentially free in Fischer carbenes. The calculated rotational barriers for Fischer carbenes are generally smaller than the rotational barrier around the C–C single bond in ethane (2.9 kcal mol^{-1}).[27] For Schrock carbenes the experimental[28] and theoretical[8f,8d,9a] rotational barriers are larger (10–20 kcal mol^{-1}), but when compared to main group analogues such as ethylene for which the rotational barrier amounts to 65 kcal mol^{-1},[29] they are also relatively small. The differences between the rotational barriers around the TM=C$_{carb}$ bond in Fischer and Schrock compounds have been traced back to the nature of π-backbonding interactions. The TM in Fischer complexes has two occupied degenerate (or almost degenerate) d$_\pi$ orbitals which allow π-backbonding in any orientation of the carbene ligand.[8c] On the other hand, the TM in Schrock complexes has no degenerate occupied d$_\pi$ orbitals and π-backbonding is only effective for one particular orientation of the complexed carbene ligand.

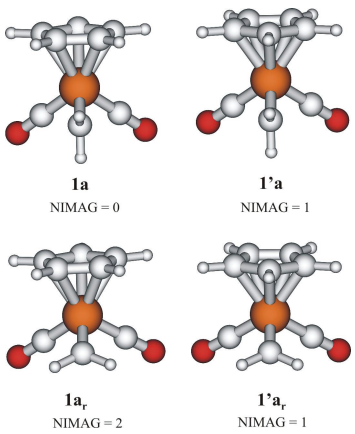

Figure 2. Optimized stationary structures of the complex $[(CO)_2(\eta^5\text{-}C_5H_5)Fe{=}CH_2]^+$.

From Table 1 it is evident that, the rotational barriers of the dimethylcarbene in **1c**–**3c** (2.1–4.3 kcal mol^{-1}) are of the order of those in Fischer carbenes, while the rotational barriers of methylidene in **1a**–**4a** (8.3–12.2 kcal mol^{-1}) approach those of Schrock

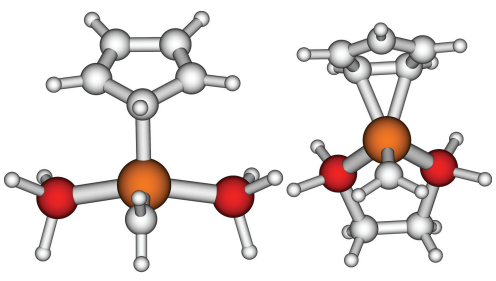

Scheme 3.

Table 1. Relative energies expressed in kcal mol^{-1}, of the optimized structures **1a-c** – **4a-c**, **1'a-c** – **4'a-c**, **1a$_r$-c$_r$** – **4a$_r$-c$_r$** and **1'a$_r$-c$_r$** – **4'a$_r$-c$_r$**

		CH_2		CF_2		CMe_2	
L1, L2		**a**	**a$_r$**	**b**	**b$_r$**	**c**	**c$_r$**
CO	**1**	0.0	10.0	0.0	4.3	0.0	3.9
	1'	1.0	**8.3**	0.7	**3.5**	2.3	**2.1**
PH_3	**2**	0.0	11.1	0.0	5.5	0.0	4.9
	2'	—	**10.0**	0.8	**5.2**	3.7	**3.4**
dhpe	**3**	0.0	**12.2**	0.0	**6.5**	0.0	4.8
	3'	1.9	—	2.1	6.9	2.7	**4.3**
PPh_3	**4**	0.0	**8.9**	0.0	**8.1**	0.0	**10.3**
	4'	1.9	11.8	5.2	10.5	5.1	14.5

compounds. The rotational barriers of difluorocarbene are between those of methylidene and dimethylcarbene (Table 1). The rotational barrier **3a$_r$** (12.2 kcal mol^{-1}, L = dhpe) is close to the experimental value of 10.4 kcal mol^{-1} obtained in NMR studies on the related (dppe)(η^5-C_5H_5)Fe=CH_2^+ complex.[18a] The experimental rotational barriers for the remaining complexes are not known. It should be noticed however, that for **1c** either a fast rotation of the dimethylcarbene around the Fe–C_{carb} bond or a stable structure with equivalent methyl groups was postulated on the basis of ^{1}H and ^{13}C NMR measurements.[15b] Taking into account that the equilibrium structure of **1c** does not have equivalent methyl groups as well as the small value of the calculated rotational barrier (2.1 kcal mol^{-1}), our data support only the first assumption. For complexes with a given L the rotational barriers of the carbenes diminish in the order :CH_2 > :CF_2 > :CMe_2 (Table 1). The only exception is calculated for **4c** for which the rotational barrier of :CMe_2 (10.3 kcal mol^{-1}) is larger than that of :CH_2 (8.9 kcal mol^{-1}) and :CF_2 (8.1 kcal mol^{-1}) (Table 1). However, taking into account the bulky nature of the PPh_3 ligands as well as that of CMe_2 in comparison with CH_2 and CF_2, leads to the conclusion that the large rotational barrier of the dimethylcarbene in **4c** is due to steric factors. From Table 1 it is seen that the replacement of the CO ligands by the poorer π-acceptor ones increases the carbene rotational barriers. Thus, for example, the rotational barriers of the difluorocarbene in **1b**–**4b** increase from 3.5 kcal mol^{-1} (L = CO) to 5.2 kcal mol^{-1} (L = PH_3), 6.5 kcal mol^{-1} (L = dhpe), and 8.1 kcal mol^{-1} (L = PPh_3). The increase of the rotational barriers in the ordering CO < PH_3 < dhpe < PPh_3 is also valid for the dimethylcarbene complexes, but the rotational barrier of methylidene in **4a** (8.9 kcal mol^{-1}; L = PPh_3) is smaller

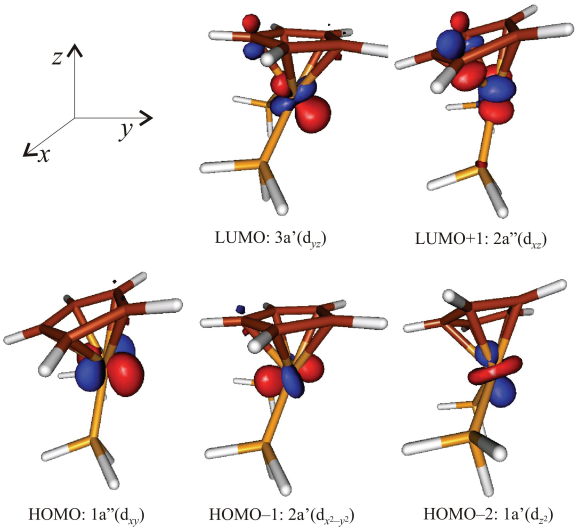

Figure 3. Valence Kohn-Sham MOs of the molecular fragment (PH_3)$_2$(η^5-C_5H_5)Fe^+ (**2**).

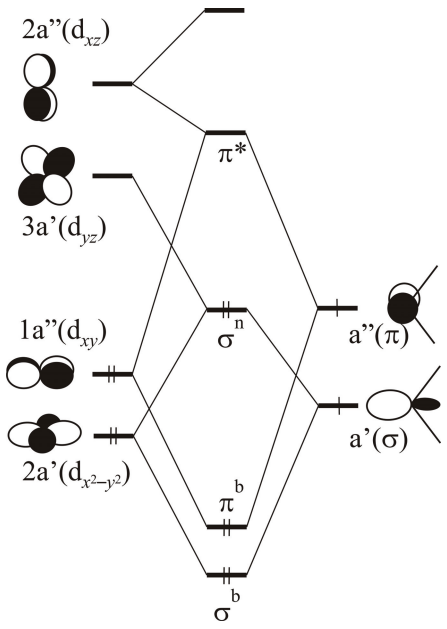

Figure 4. Simplified interaction diagram between the valence MOs of the molecular fragments L_2(η^5-C_5H_5)Fe^+ with those of a carbene CR_2 in a triplet state.

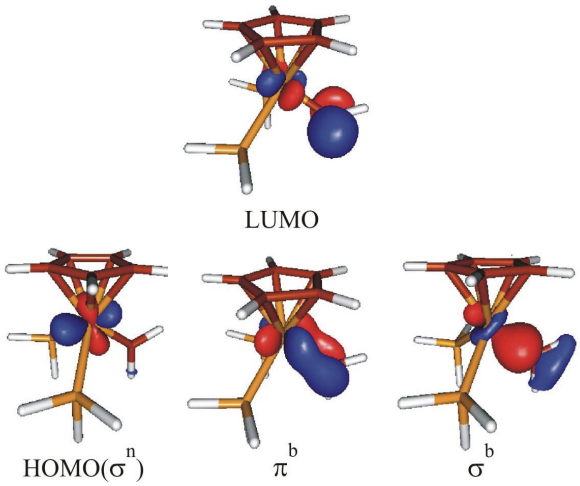

Figure 5. Valence Kohn-Sham MOs of **2a**.

than that in **2a** (10.0 kcal mol^{-1}; L = PH_3) and **3a** (12.2 kcal mol^{-1}; 2L = dhpe).

A useful way of understanding the nature of the iron-carbene interactions is to correlate the valence MOs of the corresponding molecular fragments.[30] The frontier orbitals of the metal fragments $L_2(\eta^5\text{-}C_5H_5)Fe^+$ and carbenes are well known. In $L_2(\eta^5\text{-}C_5H_5)Fe^+$ six valence electrons occupy three iron d-type levels. The LUMO and LUMO+1 are the antibonding counterpart of the iron-cyclopentadienyl bonding, both MOs have also predominant iron d-character.[30] Note, that the iron atom in the $L_2(\eta^5\text{-}C_5H_5)Fe^+$ molecular fragments has only one occupied d_π MO. The valence Kohn-Sham MOs of **2** are depicted in Figure 3 as an example. Figure 4 illustrates a simplified correlation diagram for the interactions between the valence MOs of the $L_2(\eta^5\text{-}C_5H_5)Fe^+$ fragments with those of a carbene $:CR_2$ in a triplet state.

From Figure 4 it is evident that the bonding between the iron and a carbene in a triplet state is best described in terms of three electrons three orbital interactions. As a result of the Aufbau principle, a σ and π bond is formed between the iron atom and the carbene carbon atom (Figure 4). The HOMO of the $L_2(\eta^5\text{-}C_5H_5)Fe{=}CR_2^+$ compounds is a nonbonding orbital localized at iron and LUMO is the antibonding counterpart of the Fe–C_{carb} π bond (Figure 4). For the sake of clarity the valence MOs of **2a** are depicted in Figure 5.

Table 2. Rotational barriers of the carbene ligands, ΔE_{rot} / kcal mol^{-1}, and the NPA charge q associated with the iron atom (qFe) and the ligands ($q C_5H_5$, q2L, $q CR_2$) as well as electronic population (OCC) of the NBOs describing the iron carbene carbon bonds in the global minimum structures **1a-c** – **4a-c** and the carbene rotamers **1'a$_r$-c$_r$**, **2'a$_r$-c$_r$**, **3'c$_r$**, **3a$_r$**, **3b$_r$**, and **4a$_r$-c$_r$**

L	:CR_2	Comp.	ΔE_{rot}	qC_5H_5	q2L	qFe	ΔqFe [a]	qCR_2	ΔqCR_2 [a]	OCC [b]	
										Fe–C: σ^b	Fe–C: π^b
CO	:CH_2	**1a**		0.340	0.524	–0.045		0.181		1.871 (44)	1.864 (76)
		1'a$_r$	8.3	0.322	0.472	–0.061	+0.016	0.267	–0.086	1.893 (51)	1.778 (73)
	:CF_2	**1b**		0.366	0.484	–0.131		0.281		1.903 (38)	1.857 (83)
		1'b$_r$	3.5	0.343	0.458	–0.140	+0.009	0.339	–0.058	1.879 (46)	1.755 (79)
	:CMe_2	**1c**		0.268	0.466	–0.054		0.320		1.841 (43)	1.815 (83)
		1'c$_r$	2.1	0.255	0.424	–0.080	+0.026	0.401	–0.081	1.827 (42)	—
PH_3	:CH_2	**2a**		0.143	0.886	–0.028		–0.001		1.880 (40)	1.894 (54)
		2'a$_r$	10.0	0.132	0.802	–0.030	+0.002	0.096	–0.097	1.777 (40)	1.769 (70)
	:CF_2	**2b**		0.176	0.842	–0.118		0.100		1.916 (35)	1.889 (77)
		2'b$_r$	5.2	0.155	0.792	–0.127	+0.009	0.180	–0.080	1.796 (27)	—
	:CMe_2	**2c**		0.097	0.830	–0.030		0.103		1.870 (39)	1.850 (76)
		2'c$_r$	3.4	0.088	0.740	–0.047	+0.017	0.219	–0.116	1.871 (39)	—
dhpe	:CH_2	**3a**		0.121	0.952	–0.047		–0.026		1.876 (40)	1.807 (54)
		3a$_r$	12.2	0.096	0.868	–0.041	–0.006	0.077	–0.103	1.703 (38)	1.760 (65)
	:CF_2	**3b**		0.152	0.914	–0.144		0.078		1.909 (35)	—
		3b$_r$	6.5	0.130	0.862	–0.148	+0.004	0.156	–0.078	1.907 (35)	—
	:CMe_2	**3c**		0.080	0.879	–0.054		0.095		1.856 (39)	—
		3'c$_r$	4.3	0.068	0.799	–0.061	+0.007	0.194	–0.099	1.837 (39)	—
PPh_3	:CH_2	**4a**		0.050	0.930	0.084		–0.064		1.867 (38)	1.859 (51)
		4a$_r$	8.9	0.017	0.868	0.097	–0.013	0.018	–0.082	1.920 (49)	1.782 (61)
	:CF_2	**4b**		0.085	0.878	0.007		0.030		1.904 (34)	1.890 (75)
		4b$_r$	8.1	0.054	0.772	0.079	–0.072	0.095	–0.065	1.903 (33)	—
	:CMe_2	**4c**		0.024	0.806	0.130		0.040		1.857 (37)	1.839 (73)
		4c$_r$	10.3	0.001	0.740	0.136	–0.006	0.123	–0.083	1.857 (37)	—

[a] Negative sign means decrease of electron density.
[b] Values in parentheses give contribution of iron NAOs in percents.

Table 3. Selected optimized parameters of the global minimum structures **1a-c** – **4a-c** and the carbene rotamers **1'a$_r$**–**1'c$_r$**, **2'a$_r$**–**2'c$_r$**, **3a$_r$**– **3c$_r$**, **4a$_r$**, **4'b$_r$**, and **4c$_r$**. Bond distances are given in Å, bond angles in deg

L	R	Comp.	Fe–C_{carb}	C_{carb}–R	∠R–C_{carb}–R	Fe–$C(Cp)_{avr}$	Fe–L	∠L–Fe–L	∠C_{carb}–Fe–L
CO	H	**1a**	1.798	1.100	112.6	2.149	1.791	90.7	91.8
		1'a$_r$	1.799	1.102	112.7	2.145	1.801	98.5	93.2
	F	**1b**	1.831	1.312	107.5	2.139	1.796	91.8	93.2
		1'b$_r$	1.830	1.307	107.8	2.138	1.799	95.9	93.6
	CH_3	**1c**	1.872	1.493	111.9	2.153	1.780	92.9	90.6
		1'c$_r$	1.870	1.484	115.1	2.144	1.784	95.3	94.0
PH_3	H	**2a**	1.785	1.101	110.6	2.140	2.197	91.7	90.4
		2'a$_r$	1.779	1.105	110.7	2.138	2.223	99.1	91.2
	F	**2b**	1.796	1.328	105.3	2.128	2.211	92.5	92.5
		2'b$_r$	1.788	1.330	105.6	2.127	2.224	95.7	93.8
	CH_3	**2c**	1.845	1.506	109.1	2.145	2.199	94.1	92.5
		2'c$_r$	1.830	1.498	112.5	2.133	2.218	94.5	95.4
dhpe	H	**3a**	1.785	1.102	110.0	2.137	2.185	84.1	91.1
		3a$_r$	1.782	1.106	110.4	2.142	2.199	87.1	91.8
	F	**3b**	1.790	1.329	104.8	2.126	2.199	84.6	93.1
		3b$_r$	1.789	1.333	105.2	2.127	2.202	85.9	94.0
	CH_3	**3c**	1.839	1.506	108.8	2.145	2.190	86.0	93.2
		3'c$_r$	1.834	1.499	112.2	2.135	2.203	85.9	95.1
PPh_3	H	**4a**	1.777	1.104	110.6	2.165	2.310	104.6	90.1
		4a$_r$	1.779	1.105	110.8	2.178	2.325	108.0	89.7
	F	**4b**	1.779	1.346	103.9	2.153	2.341	103.6	92.2
		4b$_r$	1.783	1.342	103.5	2.156	2.352	106.4	93.5
	CH_3	**4c**	1.834	1.514	108.2	2.174	2.361	104.0	93.5
		4c$_r$	1.845	1.505	108.4	2.167	2.380	106.2	97.5

Due to the three electron three orbital interactions, the Fe–C σ and π bonds do not have a pure covalent nature and donation and backdonation of electron density should also contribute to the bonding. From Figure 4 it is also evident that for interactions between the $L_2(\eta^5\text{-}C_5H_5)Fe^+$ fragments and carbenes in a singlet state, the Fe–C σ and π bonds primarily result from donor-acceptor interactions between the HOMO and LUMO of both molecular fragments. Compared with triplet carbenes, the Fe–C σ and π bonds resulting from interactions with carbenes in a singlet state should have a slightly more polarized nature.

The results of the NPA and NBO population analyses confirm the qualitative picture drawn from the interactions between the frontier MOs (Table 2). For the global minimum structures, except **3b** and **3c**, the optimal Lewis structure predicted by the NBO procedure has a σ and π bond between the carbene carbon atom and the iron center. The Fe–C_{carb} σ bond is polarized toward the carbon end. The polarization in the Fe–C_{CF2} σ bond is larger than that in the Fe–C_{CH2} and Fe–C_{CMe2} bonds. Thus, for example, the contributions of carbon AOs to the Fe–C_{carb} σ bond amount to 60 % for **3a**, 61 % for **3c**, and 65 % for **3b**. The polarization of the Fe–C_{carb} σ bond in **1a-c** – **4a-c** is very close to that found in MP2 investigations on the Schrock complexes F_4WCH_2 and F_4WCF_2 for which the contributions of carbon AOs to the W–C_{carb} σ bond amount to 61 % and 65 %, respectively.[10g] The polarization of the W–C_{carb} σ bond in the Fischer-type compounds $(CO)_5WCH_2$ and $(CO)_5WCF_2$ was predicted to be larger (>72 %).[10g] The Fe–C_{carb} π bond of **2a**, **3a**, and **4a** has an almost covalent nature, while that of the remaining complexes is strongly polarized toward the iron center (Table 2). Note that strong polarization of the TM–C_{carb} π bond is normally observed for Fischer-type compounds. The polarization of the Fe–C_{carb} σ and π bonds of **1a-c** – **4a-c** show also similarities to that found in recent DFT studies on the related compounds $Cp(CO)LFe{=}CHR^+$ (L = CO, PMe_3).[31] It should be noticed however, that a straightforward comparison with our results is not possible, primarily due to the in our opinion scarce and not always adequate discussion of the NBO data presented in Ref. 31.

From Table 2 it is evident that the rotation of the carbene ligands leads to the decrease of the electron population of the π bonds. Similar as for **3b** and **3c** the optimal Lewis structure of the dimethylcarbene rotamers **1'c$_r$**–**3'c$_r$** and **4c$_r$** as well of the difluorocarbene rotamers **2'b$_r$**, **3b$_r$**, and **4b$_r$** has only the Fe–C_{carb} σ bond. For these complexes the NBO population analyses suggest that the Fe–C_{carb} π bond is even more polarized, because the optimal Lewis structure has a lone-pair (d_π) orbital at iron instead of the Fe–C_{carb} π bond. In

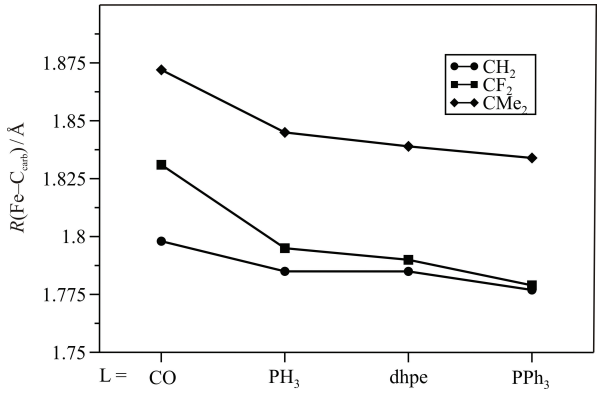

Figure 6. Graphical illustration of the optimized Fe–C_{carb} bond lengths of **1a-c** – **4a-c** as a function of the ligand L (L = CO, PH_3, dhpe, PPh_3) and the carbenes CH_2, CF_2, and CMe_2.

1a-c – **4a-c** the carbene ligand carries a positive or close to zero partial charge (between –0.06 and 0.32) which for complexes with given L increases in the order :CH_2 < :CF_2 < :CMe_2. With respect to the global minimum structures **1a-c** – **4a-c** the electron density associated with carbenes diminishes in the carbene rotamers **1'a$_r$-c$_r$**, **2'a$_r$-c$_r$**, **3'c$_r$**, **3b$_r$**, and **4a$_r$-c$_r$**. The decrease of the electron density at carbenes is accompanied by charge reorganization at iron and at the ligands L and C_5H_5 (Table 2).

The optimized Fe–C_{carb} bond lengths as well as the carbene R–C–R bond angles are not influenced by the carbene rotation (Table 3). For example, the Fe–C_{carb} bond distance of **3a** (1.785 Å) is of the same order as that of **3a$_r$** (1.782 Å) and the H–C–H bond angles are also virtually the same (110.0º (**3a**), 110.4º (**3a$_r$**)). Note that the optimized geometrical parameters of **3a** are in excellent agreement with the experimental values of the closely related compound [(dppe)(η^5-C_5Me_5)Fe=CH(Me)]$^+$ (Fe–C_{carb}: 1.785 Å *vs*. 1.787 Å; Fe–P: 2.185 Å *vs*. 2.230 Å; ∠ P–Fe–P: 84.1º *vs*. 86.2º; ∠ C_{carb}–Fe–P: 91.1º *vs*. 90.9º, (Table 3, Ref. 18b)).

From Table 3 it is seen that the iron carbene bond lengths are sensitive to the electronic nature and chemical environments of the carbene ligand. For the global minimum structures with given L, the Fe–C_{carb} bond distances increase in the order :CH_2 < :CF_2 < :CMe_2. The optimized Fe–C_{carb} bond distances of the dimethylcarbenes **1c**–**4c** range from 1.843 Å to 1.872 Å and are well separated from those of the difluorocarbenes **1b**–**4b** and the methylidene compounds **1a**–**4a** (Table 3, Figure 6). The Fe–C_{carb} distances of **1c**–**4c** approach the experimental values found for the Fischer-type thiocarbenes $(CO)_2(\eta^5\text{-}C_5H_5)Fe{=}C(H)SPh^+$ (1.88 Å) and $(CO)_2(\eta^5\text{-}C_5H_5)Fe{=}C(CH_3)SCH_3^+$ (1.94 Å).[32]

The Fe–C_{carb} bond lengths are also sensitive to the nature of the ligand L attached to iron. The replacement of the CO ligand by the PH_3, dhpe and PPh_3 ones leads to a decrease of the Fe–C_{carb} bond distance (Figure 6). The decrease of the Fe–C_{carb} distance in the ordering CO> PH_3 ≥ dhpe > PPh_3 may be traced back to the π acceptor properties of these ligands. It is clear that a poorer π-acceptor ligand attached to iron will increase backbonding from the iron center to the carbene ligand which of course will lead to a shorter Fe–C_{carb} bond and a higher carbene rotational barrier. Similar properties were also observed in the X–ray crystal structure studies on the $(CO)_2(\eta^5\text{-}C_5H_5)Fe{=}CCl_2^+$ and $(CO)(PPh_3)(\eta^5\text{-}C_5H_5)Fe{=}CF_2^+$ compounds.[33] The Fe–C_{carb} distance in the former complex of 1.808 Å decreases to 1.724 Å in the later one. A decrease of the Fe–C_{carb} bond distances was also observed in the DFT studies on the complexes $Cp(CO)_2Fe{=}CHR^+$ and $Cp(CO)(PMe_3)Fe{=}CHR^+$, for which the replacement of one CO ligand by PMe_3 shortens the Fe–C_{carb} bond distance up to 0.037 Å.[31] Table 3 shows also that the substitution of dhpe by PH_3 and PPh_3 results in an elongation of the Fe–P bonds. It is interesting to note that similar properties have been observed in theoretical studies on the $Fe(CO)_4PR_3$ and related compounds.[34]

The coordination of the carbenes **a**–**c** with the metal fragments **1**, **2'**, **3**, and **4** elongates the Fe−C(Cp) bond distances of **1a-c** – **4a-c**. Independently of the ligands L attached to iron, the largest elongation of the Fe−C(Cp) bond distances is observed in the case of the dimethylcarbene complexes and the smallest one for the difluorocarbene compounds (Tables 3 and 4). Compared to **1**, **2'**, **3**, and **4** the Fe–L bond distances of **1a-c** – **3a-c** and **4a** are shortened, while those of **4b** and **4c** are slightly elongated, most probably due to steric reasons.

The optimized L–Fe–L bond angles of **1a-c** – **4a-c** adopt similar values; they range from 90º to 94º. Compared to the free metal fragments, the L–Fe–L bond angles decrease in **1a-c**, **2a-c**, and **4a-c** and increase in **3a-c** for the chelating ligand dhpe (Tables 3 and 4). The coordination of the carbenes leads also to significant diminution of the R–C–R bond angle in the case of the methylidene and dimethylcarbene complexes, while that of **1b**–**4b** is almost the same as in :CF_2 (**b**). These properties are inherently connected to the electronic structures of the free and complexed carbenes. Like for the ground state singlet of :CF2 (**b**), the complexed in **1a-c** – **4a-c** carbenes possess closed shell electronic structures, while the ground state electronic structure of :CH2 (**a**) and :CMe2 (**c**) corresponds to the triplet state (Table 4). The optimized R–C–R angle of the triplet state of :CH_2 (**a**) (135.7º) and :CMe2 (**c**) (134.6º) diminishes to 110º–113º in **1a**–**4a** and to 108º–112º in **1c**–**4c** and approach the values calculated for the singlet states of the methylidene and dimethylcarbene (Table 4).

Table 4. Selected optimized parameters of the lowest energy molecular fragments $L_2(\eta^5\text{-}C_5H_5)Fe^+$ [L = CO (**1**), PH_3 (**2'**), PPh_3 (**4**); 2L = dhpe (**3**)] and of the carbenes $:CR_2$ [R = H (**a**), F (**b**), CH_3 (**c**)] in the singlet (S) and triplet (T) states together with the singlet-triplet splitting, ΔE(S–T) / kcal mol^{-1}. Bond distances are given in Å, bond angles in deg

L		Fe–C(Cp)$_{avr}$	Fe–L	∠L–Fe–L
CO (**1**)		2.112	1.804	94.0
PH_3 (**2'**)		2.071	2.230	98.5
dhpe (**3**)		2.080	2.205	85.8
PPh_3 (**4**)		2.092	2.325	106.0
R		C–R	∠R–C–R	ΔE(S–T)
H (**a**)	T	1.086	135.7	+16.8
	S	1.125	100.1	
CH_3 (**c**)	T	1.465	134.6	+2.2
	S	1.469	112.4	
F (**b**)	T	1.330	119.8	–50.9
	S	1.323	104.5	

Table 5. Counterpoise corrected dissociation energy D_e of the carbenes $:CR_2$ from the complexes **1a-c**, **2a-c**, **3a-c**, and **4a-c** together with the contributions from intrinsic interaction energy (ΔE_i^{CP}) and the relaxation energy of the molecular fragments $L_2(\eta^5\text{-}C_5H_5)Fe^+$ [$\Delta E_{rel}(1)$] and $:CR_2$ [$\Delta E_{rel}(2)$] in comparison with the Fe–C_{carb} bond lengths (given in Å). All energies are given in kcal mol^{-1}

	$:CR_2$	ΔE_i^{CP}	$\Delta E_{rel}(1)$	$\Delta E_{rel}(2)$	D_e	$R_{Fe-Ccarb}$
$(dhpe)(\eta^5\text{-}C_5H_5)Fe^+$ (**3**)	$:CH_2$ (**a**)	101.2	–4.0	–6.1	91.1	1.785
	$:CMe_2$ (**c**)	96.7	–4.5	–9.7	82.5	1.850
	$:CF_2$ (**b**)	72.2	–3.0	–0.7	68.5	1.790
$(PH_3)_2(\eta^5\text{-}C_5H_5)Fe^+$ (**2**)	$:CH_2$ (**a**)	100.1	–4.3	–5.5	90.3	1.785
	$:CMe_2$ (**c**)	97.4	–6.4	–11.6	79.4	1.854
	$:CF_2$ (**b**)	70.9	–3.8	–0.3	66.8	1.796
$(CO)_2(\eta^5\text{-}C_5H_5)Fe^+$ (**1**)	$:CH_2$ (**a**)	95.9	–2.4	–4.7	88.8	1.798
	$:CMe_2$ (**c**)	102.5	–2.3	–8.8	91.4	1.872
	$:CF_2$ (**b**)	67.5	–1.5	–0.5	65.5	1.831
$(PPh3)_2(\eta^5\text{-}C_5H_5)Fe^+$ (**4**)	$:CH_2$ (**a**)	91.6	–5.6	–5.7	80.3	1.777
	$:CMe_2$ (**c**)	89.2	–11.3	–9.8	68.2	1.834
	$:CF_2$ (**b**)	67.3	–6.3	–0.5	60.5	1.779

Binding Energies of the Carbene Ligands CH_2, CF_2, and CMe_2

The counterpoise corrected dissociation energies of the carbene ligands and their decomposition into intrinsic and relaxation energies are collected in Table 5. Figure 7 gives a graphical illustration of the dissociation energies as a function of the carbene substituens and the ligand L attached to iron. The dissociation processes were calculated with respect to the equilibrium ground state structures of the complexes and their molecular fragments ($^1A'$ for **1a-c** – **4a-c** and **1**–**4**, $^3B_1$ for $:CH_2$ and $:CMe_2$, and $^1A_1$ for $:CF_2$). The BSSE contamination of the dissociation energies was calculated to be negligible (< 5 %) and is not discussed.

From Table 5 and Figure 7 it is evident that for complexes with given L, except **1c**, the intrinsic dissociation energies (ΔE_i^{CP}) decrease in the order $CH_2 \geq CMe_2 >> CF_2$. Although these trends do not change when relaxation energies are added, the energetic separation of the D_e values of CMe_2 from those of CH_2 is becoming larger (Figure 7). This is mainly due to the different $\Delta E_{rel}(2)$ values of the particular carbenes and to a lesser extent to the $\Delta E_{rel}(1)$ energies of the metal fragments (Table 5). The smallest relaxation energies are calculated for $:CF_2$ (from –0.3 to –0.7 kcal mol^{-1}) and the largest ones for $:CMe_2$ (from –8.8 to –11.6 kcal mol^{-1}). The relaxation energies of the carbene ligands are mainly due to the changes of the R−C−R angles upon bond formation with the iron center. As mentioned previously, the optimized F−C−F bond angle of $:CF_2$ (104.5º) changes only little in **1b**–**4b** (103.9º–107.5º), but that of $:CMe_2$ (136.4º) and $:CH_2$ (135.7º) decreases in **1a-c** – **4a-c** by 23º– 28º.

The experimental dissociation energies of the carbene ligands in **1a-c** – **4a-c** are not known. To the best of our knowledge, experimental energies for metal carbene double bonds are only available from the ion beam experiments on naked metal carbene species, $M{=}CH_2^+$.[35]

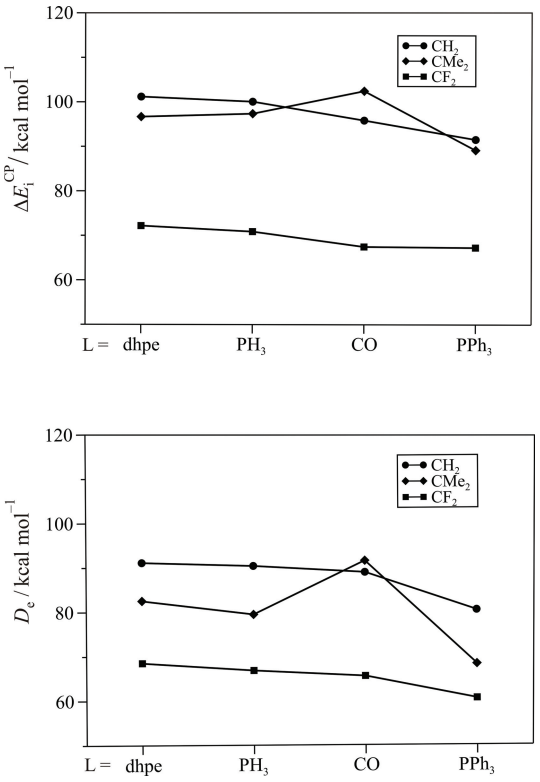

Figure 7. Graphical illustration of the counterpoise corrected intrinsic- (ΔE_i^{CP}) (top) and total dissociation energies (D_e) (bottom) of the carbene ligands CH_2, CF_2, and CMe_2 as a function of the ligand L (L = CO, PH_3, dhpe, PPh_3) attached to iron.

The authors determined the M=CH_2 bond strengths for Cr^+ through Ni^+ that range from (65 ± 7) kcal mol $^{-1}$ (M = Cr^+) to (96 ± 5) kcal mol^{-1} (M = Fe^+).[35a] In Ref. 35b a lower dissociation energy of (82 ± 5) kcal mol^{-1} was presented for Fe=CH_2^+. The calculated dissociation energies of :CH_2 in **1a**–**4a** range from 80.3 kcal mol^{-1} (**4a**) to 91.1 kcal mol^{-1} (**3a**) and are in reasonable agreement with the experimental values. It is clear, that due to the coordinatively saturated nature of the investigated complexes**,** a more detailed comparison with the experimental values of the naked species Fe=CH_2^+ is not possible for chemical reasons.

It was argued in the literature that methyl and fluorine can donate electrons into the π orbital of the carbene and that this substitutent donation competes with the back-donation from the metal fragments.[10b] As a consequence of this competition the substituted carbene ligands form weaker π-bonds than methylidene itself and obviously the total Fe−C_{carb} bond strength should be also weaker. The replacement of hydrogen by methyl or fluorine in the methylidene complexes **1a**–**4a** decreases the Fe–C_{carb} bond strengths by 9–12 kcal mol^{-1} for the dimethylcarbenes **2c**–**4c** and by 20–23 kcal mol^{-1} for the difluorocarbenes **1b**–**4b**. In **1c** the dimethylcarbene is by 2.6 kcal mol^{-1} stronger bonded to the iron than the methylidene in **1a**. This finding suggests that donor-acceptor interactions are not always the decisive factors which control the Fe−C_{carb} bond strengths. In order to verify if the ordering of the calculated D_e values is influenced by the choice of the functional and/or the basis sets we performed single-point calculations on **1a-c** by using the B97-D[23] and B3LYP[24] functionals for the BP86/TZVP optimized structures as well as we carried out BP86 geometry optimization by using larger TZVPP basis sets. With the aim of comparison analogous calculations were also carried out for **3a-c**. For the sake of clarity the calculated ΔE values are collected in Table 6.

The data from Table 6 show that the tendencies observed for the Fe=C_{carb} bond strengths are not influenced by the choice of the functional or the more flexible basis sets. This is also true for the hybrid B3LYP functional which (compared to BP86 and B97-D results) predicts weaker Fe=C_{carb} bond strengths.

The calculated weakening of the Fe–C_{carb} bond strengths {Δ[D_e(Fe=CH_2), D_e(Fe=CF_2)] = 20–23 kcal mol^{-1}]} for **1b**–**4b** is close to that obtained in DFT studies on the Fischer complexes $(CO)_5Cr{=}CH_2$ and $(CO)_5Cr{=}CF_2$ for which the Δ[D_e(Cr=CH_2), D_e(Cr=CF_2)] amounts to 24 kcal mol^{-1},[10b] as well as to that from CCSD(T) studies on analogous tungsten compounds (18 kcal mol^{-1}).[10g] It is interesting to note that the CCSD(T) Δ[D_e(W=CH_2), D_e(W=CF_2)] value for the

Table 6. Comparison of the dissociation energies ΔE of the carbenes in **1a-c** and **3a-c** calculated at several method/basis set levels

	ΔE / kcal mol^{-1} [(a)]			
	BP86/TZVP	B97-D/TZVP	B3LYP/TZVP	BP86/TZVPP
$(CO)_2CpFe{=}CH_2^+$ (**1a**)	90.1	88.9	79.5	90.0
$(CO)_2CpFe{=}CMe_2^+$ (**1c**)	92.9 (+2.8)	96.0 (+7.1)	82.5 (+3.0)	92.8 (+2.8)
$(CO)_2CpFe{=}CF_2^+$ (**1b**)	67.4 (–22.7)	65.3 (–23.6)	57.1 (–22.4)	67.1 (–22.9)
$(dhpe)CpFe{=}CH_2^+$ (**3a**)	92.1	92.1	80.7	92.2
$(dhpe)CpFe{=}CMe_2^+$ (**3c**)	84.4 (–7.7)	89.9 (–2.2)	72.6 (–8.1)	84.3 (–7.9)
$(dhpe)CpFe{=}CF_2^+$ (**3a**)	70.4 (–21.7)	69.8 (–22.3)	58.9 (–21.8)	69.7 (–22.5)

[(a)] Values in parentheses refer to relative energies with respect to those of :CH_2 [ΔE(:CR_2) – ΔE(:CH_2)].

Schrock complexes $F_4W{=}CH_2$ and $F_4W{=}CF_2$ was predicted to be about three times larger (61 kcal mol^{-1}).[10g]

The changes of bond lengths during bond-breaking or bond formation processes are often correlated with the bond strengths. From Tables 4 and 3 it is evident that the calculated Fe–C_{carb} bond strengths do not correlate directly with the Fe–C_{carb} bond lengths. Thus, for example, with respect to **1c**–**4c**, the Fe–C_{carb} bonds of **1b**–**4b** are weaker despite shorter Fe–C_{carb} bond lengths.

The substitution of PH_3 by PPh_3 weakens the Fe–C_{carb} bond by 10.0 kcal mol^{-1} (:CH_2), 11.2 kcal mol^{-1} (:CMe_2), and 6.3 kcal mol^{-1} (:CF2). Since, as discussed in the previous section, significant differences are also calculated for the carbene rotational barriers and the Fe–C_{carb} bond distances, the PH_3 ligand can only be considered with caution as a good model for PPh_3 in computational studies.

Finally, the calculations predict that the carbene ligands in **1a-c** – **4a-c** are strongly bound to the iron than CO in the ironpentacarbonyl complex[36]. From Table 5 it is evident that among the investigated complexes even the weakest Fe–C_{CF2} bond calculated for **4b** (60.5 kcal mol^{-1}) is stronger than the experimental first bond dissociation of CO from $Fe(CO)_5$ (41.6 ± 3.1 kcal mol^{-1}).[37]

CONCLUSION

The molecular and electronic structures of the cationic carbene complexes $[L_2(\eta^5\text{-}C_5H_5)Fe{=}CR_2]^+$ (L = CO (**1**), PH_3 (**2**), dhpe (**3**), PPh_3 (**4**); R = H (**a**), F (**b**), CH_3 (**c**)) were studied by using the DFT/BP86 method and extended basis sets. The interactions between the metal fragments $L_2(\eta^5\text{-}C_5H_5)Fe^+$ and carbenes in a triplet state are best described in terms of three electron three orbital interactions and those of carbenes in a singlet state primarily result from donor-acceptor interactions between the HOMO and LUMO of both molecular fragments. For both, the singlet and triplet carbenes, a polarized σ and π bonds are formed between the carbene carbon atom and the iron center. The rotational barriers of the carbenes around the Fe=C_{carb} bond (ΔE_{rot}) as well as the character of the Fe=C_{carb} bonds are sensitive to the carbene substituents and to the ligands L attached to iron. The most important conclusions are:

For complexes with given L the values of ΔE_{rot} diminishes in the order: $CH_2 > CF_2 > CMe_2$ and an inverse ordering was obtained for the Fe=C_{carb} bond distances. The ΔE_{rot} of dimethylcarbene (2.1–4.3 kcal mol^{-1}) are close to those of Fischer carbenes for which the rotational barriers are usually smaller than 3 kcal mol^{-1}. The ΔE_{rot} of methylidene (8.3–10.0 kcal mol^{-1}) approach the experimental and/or theoretical values known for typical Schrock-carbenes. The replacement of the CO ligand by poorer π-acceptor ligand increases the values of ΔE_{rot} in the order: CO < PH_3 < dhpe < PPh_3 and diminishes the Fe=C_{carb} bond distances in the same order. All these properties can be traced back to the character of the Fe → C_{carb} π-backbonding interactions and their competitions with the Fe → L and R → C_{carb} π-interactions.

The optimized equilibrium structure of **1c** does not have equivalent methyl groups. The small value of ΔE_{rot} (2.1 kcal mol^{-1}) suggests that in **1c** a fast rotation of the dimethylcarbene occurs.

For complexes with given L, the binding energies (D_e) of the carbenes decrease in the order: $CH_2 > CMe_2 > CF_2$. The calculated weakening of the Fe−C_{carb} bond strengths {$\Delta[D_e(Fe{=}CH_2), D_e(Fe{=}CF_2)]$} of 20–23 kcal mol^{-1} is very close to those obtained in DFT and CCSD(T) studies on the Fischer complexes of chromium and tungsten[10b,g] and differs much from the bond weakening calculated in the case of Schrock-type carbenes.[10g] The calculated D_e values of all investigated carbenes are larger than the first dissociation energy of CO from the pentacarbonyliron complex. This finding suggests that the investigated compounds should be thermodynamically stable and that their high reactivity is due to kinetic factors.

Since the substitution of the PH_3 ligand by the PPh_3 one leads to significant changes of (i) the Fe=C_{carb} bond strengths, (ii) the carbene rotational barriers, and (iii) the Fe=C_{carb} bond distances the PH_3 ligand can only be considered with caution as a good model for PPh_3 in computational studies.

Acknowledgements. Support of this work from the Deutsche Forschungsgemeinschaft in the framework of the SFB 424 ("Molekulare Orientierung als Funktionskriteruim in chemischen Systemen") is gratefully acknowledged.

REFERENCES

1. (a) A. Maasböl and E. O. Fischer, *Angew. Chem*. **76** (1964) 645−645; *Angew. Chem., Int. Ed*. **3** (1964) 580−581; (b) R. R. Schrock, *J. Am. Chem. Soc*. **96** (1974) 6796−6797.
2. (a) K. H. Dötz, H. Fischer, P. Hofmann, F. R. Kreisel, U. Schubert, and K. Weiss, *Transition Metal Carbene Complexes*, VCH, Weinheim, 1983; (b) R. R. Schrock, *Chem. Rev*. **102** (2002) 145–179; (c) J. W. Herndon, *Coord. Chem. Rev*. **10** (2007) 1158−1258 and references cited.
3. (a) K. J. Ivin and J. C. Mol, *Olefin Metathesis and Metathesis Polymerization*, Academic Press, London, 1997; (b) R. H. Grubbs and S. Chang, *Tetrahedron* **54** (1998) 4413−4450; (c) A. Fürstner (Ed.), *Alkene Metathesis in Organic Synthesis*, Springer-Verlag, Berlin, 1999; (d) F. Zaragoza Dörwald, *Metal Carbenes in Organic Synthesis*, Wiley-VCH, Weinheim, 1999.

4. (a) D. Mansuy, *Pure Appl. Chem*. **52** (1980) 681−690; (b) P. R. Oritz de Montellano (Ed.), *Cytochrome P-450*, Plenum, New York, 1986; (c) Y. Li, J.-S. Huang, Z.-Y. Zhou, C.-M. Che, and X.-Z. You, *J. Am . Chem. Soc*. **124** (2002) 13185−13193 and references cited.
5. (a) P. W. Jolly and R. Pettit, *J. Am. Chem. Soc*. **88** (1966) 5044−5045; (b) M. Brookhart and W. B. Studabaker, *Chem. Rev*. **87** (1987) 411−432; M. P. Doyle and D. C. Forbes, *Chem. Rev*. **98** (1998) 911−936; (c) Q. Wang, F. H. Försterling, and M. M. Hossain, *J. Organomet. Chem*. **690** (2005) 6238−6246; (d) G. Danzinger and K. Kirchner, *Organometallics* **23** (2004) 6281−6287.
6. (a) R. R. Schrock, *Acc. Chem. Res*. **12** (1979) 98−104; (b) W. A. Nugent and J. M. Mayer, *Metal-Ligand Multiple Bonds*, Wiley, New York, 1988.
7. (a) T. F. Block, R. F. Fenske, and C. P. Casey, *J. Am. Chem. Soc*. **98** (1976) 441−443; (b) T. F. Block and R. F. Fenske, *J. Am. Chem. Soc*. **99** (1977) 4321−4330; (c) B. E. R. Schilling, R. Hoffmann, and D. L. Lichtenberger, *J. Am. Chem. Soc*. **101** (1979) 585−591; (d) R. J. Goddard, R. Hoffmann, and E. D. Jemmis, *J. Am. Chem. Soc*. **102** (1980) 7667−7676; (e) F. Volatron and O. Eisenstein, *J. Am. Chem. Soc*. **108** (1986) 2173−2179.
8. (a) A. K. Rappe and W. A. Goddard III, *J. Am. Chem. Soc*. **99** (1977) 3966−3968; (b) D. Spangler, J. J. Wendolski, M. Dupuis, M. M. L. Chen, and H. F. Schaeffer III, *J. Am. Chem. Soc*. **103** (1981) 3985−3990; (c) H. Nakatsuji, J. Ushio, S. Han, and T. Yonezawa, *J. Am. Chem. Soc*. **105** (1983) 426−434; (d) J. Ushio, H. Nakatsuji, and T. Yonezawa, *J. Am. Chem. Soc*. **106** (1984) 5892–5901; (e) D. S. Marynick and C. M. Kirkpatrick, *J. Am. Chem. Soc*. **107** (1985) 1993−1994; (f) T. R. Cundari and M. S. Gordon, *J. Am. Chem. Soc*. **113** (1991) 5231−5243; (g) T. R. Cundari and M. S. Gordon, *J. Am. Chem. Soc*. **114** (1992) 539−548; T. R. Cundari and M. S. Gordon, *Organometallics* **11** (1992) 55−63.
9. (a) T. E. Taylor and M. B. Hall, *J. Am. Chem. Soc*. **106** (1984) 1576−1584; (b) E. A. Carter and W. A. Goddard III, *J. Am. Chem. Soc*. **108** (1986) 4746−4754; (c) A. Márkez and J. Fernández Sanz, *J. Am. Chem. Soc*. **114** (1992) 2903−2909; (d) C.-C. Wang, Y. Wang, H.-J. Liu, K.-J. Lin, L.-K. Chou, and K.-S. Chan, *J. Phys. Chem*. **101** (1997) 8887−8901; (e) G. Chung and M. S. Gordon, *Organometallics* **22** (2003) 42−46.
10. (a) H. Jacobsen, G. Schreckenbach, and T. Ziegler, *J. Phys. Chem*. **98** (1994) 11406−11410; (b) H. Jacobsen and T. Ziegler, *Organometallics* **14** (1995) 224−230; (c) H. Jacobsen and T. Ziegler, *Inorg. Chem*. **35** (1996) 775−783; (d) A. W. Ehlers, S. Dapprich, S. F. Vyboishchikov, and G. Frenking, *Organometallics* **15** (1996) 105−117; (e) N. Fröhlich, U. Pidun, M. Stahl, and G. Frenking, *Organometallics* **16** (1997) 442−448; (f) M. Torent, M. Duran, and M. Solà, *Organometallics* **17** (1998) 1492−1501; (g) S. F. Vyboishchikov and G. Frenking, *Chem. Eur. J*. **4** (1998) 1428−1438; (h) G. Frenking and N. Fröhlich, *Chem. Rev*. **100** (2000) 717−774; (i) M. Cases, G. Frenking, M. Duran, and M. Solà, *Organomettalics* **21** (2002) 4182−4191; (j) M.-T. Lee and C.-H. Hu, *Organometallics* **23** (2004) 976−983; (k) L. Andrew and H.−G. Cho, *Organometallics* **25** (2006) 4040–4053.
11. (a) I. Dálmazio and H. A. Duarte, *J. Chem. Phys*. **115** (2001) 1747−1756; (b) I. Vidal, S. Melchor, and J. A. Dobado, *J. Phys. Chem. A* **109** (2005) 7500−7508.
12. (a) M. J. S. Dewar, *Bull. Soc. Chim. Fr*. **18** (1951) C71-C79; (b) J. Chatt and L. A. Duncanson, *J. Chem. Soc*. (1953) 2939−2947.
13. A. F. Hill, W. R. Roper, J. M. Waters, and A. H. Wright, *J. Am. Chem. Soc*. **105** (1983) 5939−5940.
14. (a) S. E. Kegley, M. Brookhart, and G. R. Husk, *Organometallics* **1** (1982) 760−762; (b) W. Tam, G. Lin, W. Wong, W. A. Kiel, V. K. Wong, and J. A. Gladysz, *J. Am. Chem. Soc*. **104** (1982) 141−152; (c) S. Brandt and P. Helquist, *J. Am. Chem. Soc*. **101** (1979) 6473−6475.
15. (a) C. P. Casey, W. H. Miles, H. Tukada, and J. M. O'Connor, *J. Am. Chem. Soc*. **104** (1982) 3761−3761; (b) C. P. Casey, W. H. Miles, and H. Tukada, *J. Am. Chem. Soc*. **107** (1985) 2924−2931.
16. (a) M. Brookhart and G. O. Nelson, *J. Am. Chem. Soc*. **99** (1977) 6099−6101; (b) M. Brookhart, J. R. Tucker, and G. R. Husk, *J. Organomet. Chem*. **193** (1980) C23-C26.
17. M. Brookhart, W. B. Studabaker, and G. R. Husk, *Organometallics* **4** (1985) 943−944.
18. (a) M. Brookhart, J. R. Tucker, T. C. Flood, and J. Jensen, *J. Am. Chem. Soc*. **102** (1980) 1203−1205; (b) V. Mahias, S. Cron, L. Toupet, and C. Lapinte, *Organometallics* **15** (1996) 5399−5408.
19. R. Ahlrichs, M. Bär, H.-P. Baron, S. Bauernschmitt, S. Böcker, P. Deglmann, M. Ehrig, K. Eichkorn, S. Elliot, F. Furche, F. Haase, M. Häser, H. Horn, C. Hättig, C. Huber, U. Huniar, M. Kattannek, A. Köhn, C. Kölmel, M. Kollwitz, K. May, C. Ochsenfeld, H. Öhm, H. Patzelt, O. Rubner, A. Schäfer, U. Schneider, M. Sierka, O. Treutler, B. Unterreiner, M. von Arnim, F. Weigend, P. Weis, H. Weiss, *TURBOMOLE* (Vers. 5.7), University of Karlsruhe, Karlsruhe, Germany, 2005.
20. (a) R. G. Parr and W. Yang, *Density Functional Theory of Atoms and Molecules*, Oxford University Press, New York, 1989; (b) W. Koch and M. C. Holthausen, *A Chemist's Guide to Density Functional Theory*, Wiley-VCH, Weinheim, 2000.
21. (a) A. D. Becke, *Phys. Rev. A* **38** (1988) 3098−3100; (b) J. P. Perdew, *Phys. Rev. B* **33** (1986) 8822−8824.
22. (a) K. Eichkorn, O. Treutler, H. Öhm, M. Häser, and R. Ahlrichs, *Chem. Phys. Lett*. **242** (1995) 652−660; (b) O. Treutler and R. Ahlrichs, *J. Chem. Phys*. **102** (1995) 346−354.
23. S. Grimme, *J. Comput. Chem.* **27** (2006) 1787−1799.
24. (a) A. D. Becke, *J. Chem. Phys*. **98** (1993) 5648−5652: (b) C. Lee, W. Yang and R. G. Parr, *Phys. Rev. B* **37** (1988) 785−789.
25. S. F. Boys and F. Bernardi, *Mol. Phys*. **19** (1970) 553−566.
26. (a) J. P. Foster and F. Weinhold, *J. Am. Chem. Soc*. **102** (1980) 7211−7218; (b) A. E. Reed and F. Weinhold, *J. Chem. Phys*. **78** (1983) 4066−4073; (c) A. E. Reed, R. B. Weinstock, and F. Weinhold, *Chem. Rev*. **88** (1988) 899−926; (c) J. E. Carpenter and F. Weinhold, *J. Mol. Struct*. (*THEOCHEM*) **161** (1988) 41−62.
27. J. P. Lowe, *Prog. Phys. Org. Chem*. **6** (1968) 1−80.
28. (a) J. D. Fellmann, G. A. Rupprecht, C. D. Wood, and R. R. Schrock, *J. Am. Chem. Soc*. **100** (1978) 5964−5966; (b) J. L. Brumaghim and G. S. Girolami, *Chem. Commun*. (1999) 953−954.
29. J. E. Douglas, B. S. Rabinovitsch, and F. S. Looney, *J. Chem. Phys*. **23** (1955) 315−323.
30. T. A. Albright, J. K. Burdet, and M.-H. Whangbo, *Orbital Interactions in Chemistry*, Wiley, New York, 1985.
31. Q. Meng, F. Wang, X. Qu, J. Zhou, and M. Li, *J. Mol. Struct. (THEOCHEM)* **815** (2007) 157−163.
32. C. Knors, G.-H. Kuo, J. W. Lauher, C. Eigenbrot, and P. Helquist, *Organometallics* **6** (1987) 988−995.
33. A. M. Crespi and D. F. Shriver, *Organometallics* **4** (1985) 1830−1835.
34. (a) Ò. Gonzáles-Blanco and V. Branchadell, *Organometallics* **16** (1997) 5556−5562; (b) M. Piacenza, J. Rakow, I. Hyla-Kryspin, and S. Grimme, *Eur. J. Inorg. Chem*. (2006) 213−221.
35. (a) P. B. Armentrout, L. F. Halle, and J. L. Beauchamp, *J. Am. Chem. Soc*. **103** (1981) 6501−6502; (b) R. L. Hettich and B. S. Freiser, *J. Am. Chem. Soc*. **108** (1986) 2537−2540.
36. I. Hyla-Kryspin and S. Grimme, *Organometallics* **23** (2004) 5581−5592 and references cited.
37. K. E. Lewis, D. M. Golden and G. P. Smith, *J. Am. Chem. Soc*. **106** (1984) 3905−3912.

SAŽETAK

DFT studij molekularne i elektronske strukture kationskih karbenskih kompleksa $[L_2(\eta^5\text{-}C_5H_5)Fe{=}CR_2]^+$ (L = CO, PH_3, dhpe, PPh_3; R = H, F, CH_3)

Isabella Hyla-Kryspin, Christian Mück-Lichtenfeld i Stefan Grimme

Organisch-Chemisches Institut der Universität Münster, Corrensstr. 40, D-48149 Münster, Germany

Za komplekse navedene u naslovu diskutira se o rezultatima DFT računa za sljedeća svojstva: (i) molekularne i elektronske strukture, (ii) rotacijske barijere karbena oko Fe=C_{carb} veze (ΔE_{rot}) i (iii) vezne energije karbena (D_e). U slučajevima gdje je to moguće, izračunata svojstva veza Fe=C_{carb} uspoređena su s ranijim teorijskim i eksperimetnalnim podacima za neke prototipne karbenske komplekse klasificirane kao Fischer- ili Schrock-tipove spojeva. Pokazano je kako su rotacijske barijere karbena, duljine i jakosti veza Fe–C_{carb} osjetljive na karbenski supstituent i ligande vezane na željezo. Za komplekse s navedenim ligandima (L) vrijednosti ΔE_{rot} opadaju u slijedu: CH_2 > CF_2 > CMe_2, dok je obrnuti redoslijed dobiven uz smanjenje duljine veze Fe=C_{carb}. Vrijednosti ΔE_{rot} dimetilkarbena blizu su vrijednosti spojeva Fischer-tipa, dok se one metilidena približavaju vrijednostima tipičnim za karbene Schrock-tipa. Zamjena CO liganda s lošijim π-akceptorskim ligandom povećava ΔE_{rot} vrijednosti u sljedećem nizu: CO < PH_3 < dhpe < PPh_3 i smanjuje duljine veza Fe–C_{carb} u istom redosljedu. Vezne energije (D_e) karbena veće su od prve energije disocijacije za CO u kompleksu pentakarbonilželjezo. Za komplekse s danim ligandom (L), osim jednog, D_e vrijednosti opadaju u slijedu: CH_2 > CMe_2 > CF_2. Svojstva istraživanih spojeva ovise o karakteru Fe → C_{carb} π-povratnih veznih interakcija i njihove kompeticije sa Fe → L i R → C_{carb} π-interakcijama. Također je pokazano da se PH_3 ligand samo uz veliki oprez može koristiti kao pogodan model za PPh_3 ligand u računskim studijama.